

## Nonlinear lattice excitations in charge-fluctuating systems

A. Dobry, A. Greco, R. Migoni, and M. Stachiotti

*Instituto de Física Rosario, Universidad Nacional de Rosario,*

*Bv. 27 de Febrero 210 Bis, 2000 Rosario, Argentina*

(Received 9 July 1992; revised manuscript received 5 October 1992)

The coupling of ionic charge fluctuations to lattice dynamics is studied by means of a breathing shell model with a nonlinear core-shell potential at the fluctuating ion. A molecular-dynamics simulation of the dynamical structure factor is performed for a one-dimensional diatomic model. Several qualitative differences with the structure expected from harmonic dynamics are found. Besides a softening and broadening of the breathing phonon peak with decreasing temperature, a quasistatic peak appears at short wavelengths. This occurs approximately below a temperature at which the breathing phonon becomes broadest and the softening reverses. An additional finite-frequency nonphononic structure appears at low temperature. We interpret these results in terms of nonlinear excitations of the model.

### I. INTRODUCTION

Variations of the effective ionic radius due to localized charge-density fluctuations in mixed valence compounds are known to couple with lattice dynamics, thus producing strong anomalies in the phonon dispersion curves.<sup>1</sup> We can cite, for example, the unusual temperature dependence of breathing-type motions around the valence fluctuating ion and the appearance of additional branches in the phonon spectrum.<sup>2,3</sup> This last feature has also been recently observed in the high- $T_c$  compound  $\text{La}_2\text{CuO}_4$ ,<sup>4</sup> where it may be also related to Cu charge fluctuations.<sup>5</sup>

The couplings of variations of ionic radius with lattice vibrations has been simulated through the breathing shell model.<sup>6</sup> The valence fluctuations have been considered to give rise to a nonlinear core-shell coupling at the fluctuating ion.<sup>7</sup> A local double-well potential can be understood as simulating the energy barrier between the two charge states of the ion.

In this work we shall consider a diatomic chain with a quartic double-well core-shell interaction at one of the ions. With the aim to obtain the true dynamical response without any linearization procedure, we shall calculate the dynamical structure factor from a molecular-dynamics (MD) simulation. We shall look for the effects of the nonlinear interaction in the phonon as well as for the appearance of additional features generated by the nonlinear dynamics.

### II. MODEL AND CALCULATION

The potential energy for a diatomic chain where one of the units is composed of a compressible shell coupled to a core by a quartic double-well potential  $V(w) = -\frac{1}{2}g_2w^2 + \frac{1}{4}g_4w^4$  ( $g_2 > 0$ ,  $g_4 > 0$ ) is given by

$$\Phi = \sum_n \frac{S}{2} \{ [u_1(n) + w(n) - u_2(n)]^2 + [u_1(n) - w(n) - u_2(n-1)]^2 \} + V(w), \quad (1)$$

where  $u_1(n)$  denotes the core displacements and  $w(n)$  denotes a variation of the shell radius at ion type 1.  $S$  is the interionic force constant between the shell of ion 1

and rigid ion 2.

With the purpose of simplifying the numerical analysis of the problem, it is convenient to write the equations in terms of dimensionless quantities:  $\tilde{t} = (g_2/m_2)^{1/2}t$ ,  $M = m_1/m_2$ , and  $F = S/g_2$ . Displacements  $U$  and  $W$  are measured in units of  $w_0 = (g_2/g_4)^{1/2}$ , which represents the minimum of  $V(w)$ . Therefore, we obtain the following equations of motion:

$$M\ddot{U}_1(n) = F[U_2(n) + U_2(n-1) - 2U_1(n)], \quad (2a)$$

$$\ddot{U}_2(n) = F[U_1(n+1) - W(n+1) + U_1(n) + W(n) - 2U_2(n)], \quad (2b)$$

$$0 = F[U_2(n) - U_2(n-1) - 2W(n)] + W(n) - W(n)^3. \quad (2c)$$

The last equation represents the adiabatic condition for the movement of the massless shell. The nonlinearity in  $W$  in this constraint between  $U$  and  $W$  is the origin of a nonlinear dynamics for the cores. The cubic equation (2c) can be resolved for  $W(n)$  and replaced in Eqs. (2a) and (2b). It can be seen that the condition for  $W(n)$  to have only one real root for any  $U_2(n)$  is  $F > \frac{1}{2}$ . In the forthcoming analysis we assume this condition.

Due to the nonlinear interaction  $V(w)$  the effective potential  $\Phi[u, w(u)]$  may have several configuration minima  $\{u\}_i$ . It has been shown for rigid-ion models with competitive nearest- and next-nearest-neighbor interactions that the existence of these configurations lead to structures in the static response.<sup>8</sup> Therefore, as will become apparent in the next section, it is useful to consider some analytic solutions of Eqs. (2) in the static case  $\dot{U}_k(n) = 0$ . From these equations it is possible to obtain a system involving  $P_n = U_2(n) - U_2(n-1)$ , and  $W(n)$ . Equations (2a) and (2b) lead to

$$P_{n+1} - 2W(n+1) = P_n - 2W(n) = \beta = \text{const}, \quad (3)$$

while (2a) and (3) lead to

$$-W^3(n) + W(n) + \beta F = 0. \quad (4)$$

Equation (4) can take three real roots when  $\beta^2 F^2 \leq \frac{4}{27}$  and

only one in the other case. The latter is not a physical solution because it implies  $P_n = \text{const}$  and therefore infinite energy. In the former case it is possible to construct different periodic solutions. In Table I we show solutions with period  $l$  for the simplest case  $\beta=0$ . We also include the energy per cell  $E_l$  in the  $l$ th configuration.  $l=1$  corresponds to the homogeneous solution. The configuration with  $l=2$  is the absolute minimum for the potential energy and corresponds to the breathing pattern displacement. The position of the cores in every configuration is such that all the nearest-neighbor springs in the chain are not stretching. Analogous periodic solutions may be obtained from different values of  $\beta$ .

The study of self-consistent solutions of the linearized system will help with the analysis of the numerical results obtained by MD simulations. To this purpose we approximate  $W(n)^3 \cong 3\langle W^2 \rangle W(n)$  in Eq. (2c). Thus we can eliminate  $W(n)$  from Eqs. (2a) and (2b) and obtain the following phonon dispersion relations:

$$\frac{1}{F}\omega_{o,a}^2(q) = \left[ \frac{1}{M} + 1 - 2\alpha \sin^2 \frac{qa}{2} \right] \pm \left[ \left[ \frac{1}{M} - 1 + 2\alpha \sin^2 \frac{qa}{2} \right]^2 + \frac{4}{M} \cos^2 \frac{qa}{2} \right]^{1/2} \quad (5)$$

with

$$\alpha = \frac{F}{2F - 1 + 3\langle W^2 \rangle}.$$

$\omega_o$  and  $\omega_a$  denote the optic and acoustic branch, respectively. For  $M > B$ , with

$$B = 1 + \frac{2F}{3\langle W^2 \rangle - 1},$$

the zone boundary frequencies are  $\omega_a^2(\pi/a) = 2F/M$  and  $\omega_o^2(\pi/a) = 2F/B$ . In this case the  $\omega_o(\pi/a)$  mode is a symmetric motion of ions 2 which compress and expands the shell of ion 1 (breathing mode). For  $M < B$  the previ-

ous expressions are interchanged and the acoustic mode becomes the breathing one. Instead of calculating  $\langle W^2 \rangle$  fully self-consistent, it will be obtained from the MD simulation.

The nonlinear dynamics will become more apparent the higher the double-well potential barrier is relative to the intersite coupling. This corresponds to a low  $F$ . Therefore, we take  $F=0.51$ , which leads  $B \cong 1.5$ . Finally, we take a relative mass  $M=32$  in order to get a breathing optic mode about four times higher than the acoustic mode.

### III. RESULTS AND DISCUSSION

The MD simulation is performed for a chain of 1000 unit cells with periodic boundary conditions. The shell coordinate  $W$  is obtained from Eq. (2c) in each iteration step as explained previously. The runs were performed for  $2^{14}$  steps after the zero of time, using a step size of 0.3. Then the space-time Fourier transform of the displacement-displacement correlation function is computed. This quantity gives the leading approximation to the dynamical structure factor  $S(q, \omega)$ . Figure 1 shows  $S(q, \omega)$  for  $q=3\pi/4a$  at three different temperatures, which is measured in units of  $g_2^2/g_4k_B$ . A reduced temperature  $T=0.25$  corresponds to the double-well energy barrier. At a high temperature ( $T=3.14$ ) there is a well-defined acoustic phonon and a broader optic peak. The position of the acoustic peak is in quite good coincidence with the self-consistent values indicated by the arrow and the optic phonon peak is somewhat lower than the self-consistent value, which is an effect of the anharmonicity. The intensity scale is such that the absolute maximum of the spectrum is set equal to 1. The frequency unit is  $2\pi/\tilde{t}_{\text{tot}}$ , where  $\tilde{t}_{\text{tot}}$  is the dimensionless total running time. As the temperature is lowered at  $T=0.15$  the optic peak becomes very broad and its maximum shifts to a lower frequency. At this temperature, where the mean energy per particle is slightly below the double-well barrier, the nonlinear dynamics produces a great width of the mode related to the breathing motion. At a still lower temperature,  $T=0.038$ , the optic peak becomes again sharper and its maximum shifts again to higher frequencies. Now from the MD simulation it results in  $\langle W^2 \rangle \cong 1$ , which means that the mean position of the shell is approximately the minimum of the double-well potential  $V(W)$ . In fact, the position of the optic peak coincides with the frequency obtained by linearizing the potential around  $W=1$ . A similar behavior is obtained for the structure factor at the zone boundary  $q=\pi/a$ , shown in Fig. 2. In this case the broad structure appearing at an intermediate temperature survives partially at a low temperature, below the optic peak. This feature will be analyzed more in detail later on. Figure 3 shows the temperature behavior of the optic peak maximum for both  $q$  values analyzed previously. Here it is clearly seen that the breathing mode softens with decreasing temperature only up to a finite value and then hardens again. The minimum occurs at a temperature nearly equal to the double-well barrier. This temperature behavior of the soft mode has also been found in a  $\phi^4$  chain.<sup>9</sup> In spite of

TABLE I. Static solutions with different periods  $l$  for the case  $\beta=0$ .  $w(n)$  is the shell coordinate of the configuration.  $E_l$  is the energy per unit cell.

$l$	$w(n)$	$E_l$
1	0	0
2	$(-1)^n$	$-\frac{1}{4}$
3	$\frac{2}{\sqrt{3}} \text{sen } \frac{2}{3}\pi n$	$-\frac{1}{6}$
4	$\cos \frac{\pi}{2} n$	$-\frac{1}{8}$
6	$\frac{2}{\sqrt{3}} \text{sen } \frac{\pi}{3} n$	$-\frac{1}{6}$
$\vdots$		
	$w_0 = w_T = w_{2T+1} = 0$	
$2T$	$w_1 = w_2 = \dots = w_{T-1} = 1$	$-\frac{1}{4}(1-1/T)$
	$w_{T+1} = w_{T+2} = \dots = w_{2T} = -1$	

the fact that the one-dimensional system cannot reach long-range order, the low-temperature hardening is related to the local dynamics of the particles in one of the double-well minima. This temperature behavior has also been found by Miura and Bilz<sup>7</sup> for the same model by coupling self-consistent phonons to exact nonlinear solutions. This allowed us to explain the anomalous temperature behavior of a longitudinal zone-boundary optic mode in  $\text{Sm}_{0.75}\text{Y}_{0.25}\text{S}$ .

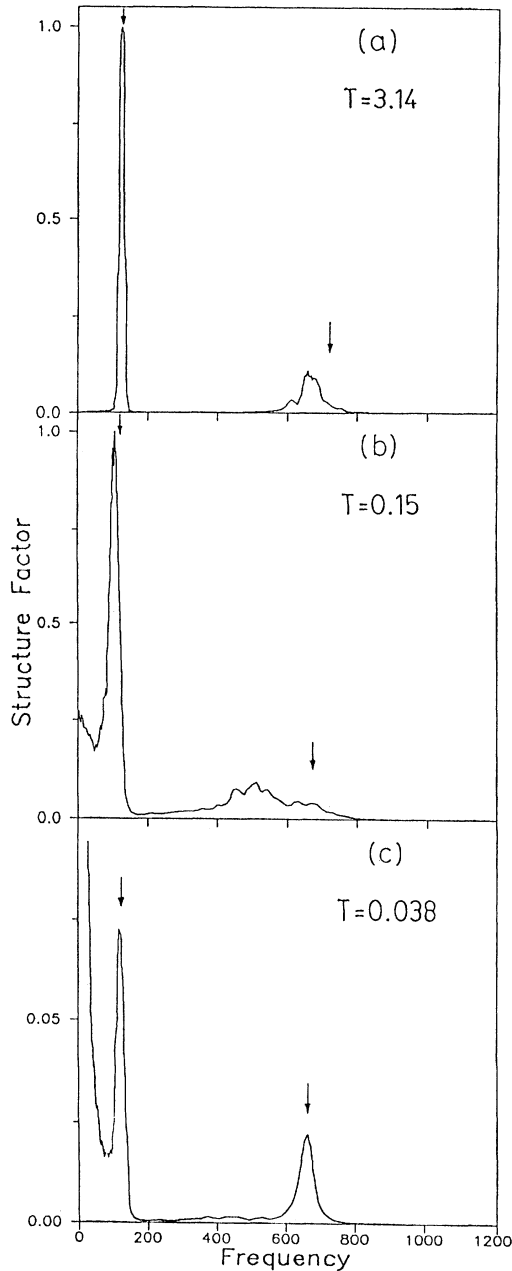


FIG. 1. Dynamical structure factor from MD simulations at  $q = \frac{3}{4}(\pi/a)$  for three values of other dimensionless temperature  $T$ . The results of a self-consistent phonon approximation are indicated by the arrows. To get rid of finite-time diffraction effects, the function was smoothed using a Gaussian.

A remarkable fact observed in Figs. 1 and 2 is the appearance of an intense peak at  $\omega = 0$  for temperatures approximately below the double-well energy barrier. This is approximately also the temperature for which the optic phonon peak becomes broader and reaches its minimum value. This peak is thinner and higher the lower the temperature is. It is not present near  $q = 0$ , reaches an intensity maximum at  $q \cong \pi/4a$ , and then decreases drastically towards the zone boundary. The low-frequency characteristic of this peak suggests that it is the quasistatic response of the lattice at stable configurations corresponding to the minima of the potential. In addition, its appearance for  $q \neq 0$  indicates that these configurations have periods which do not coincide with the lattice con-

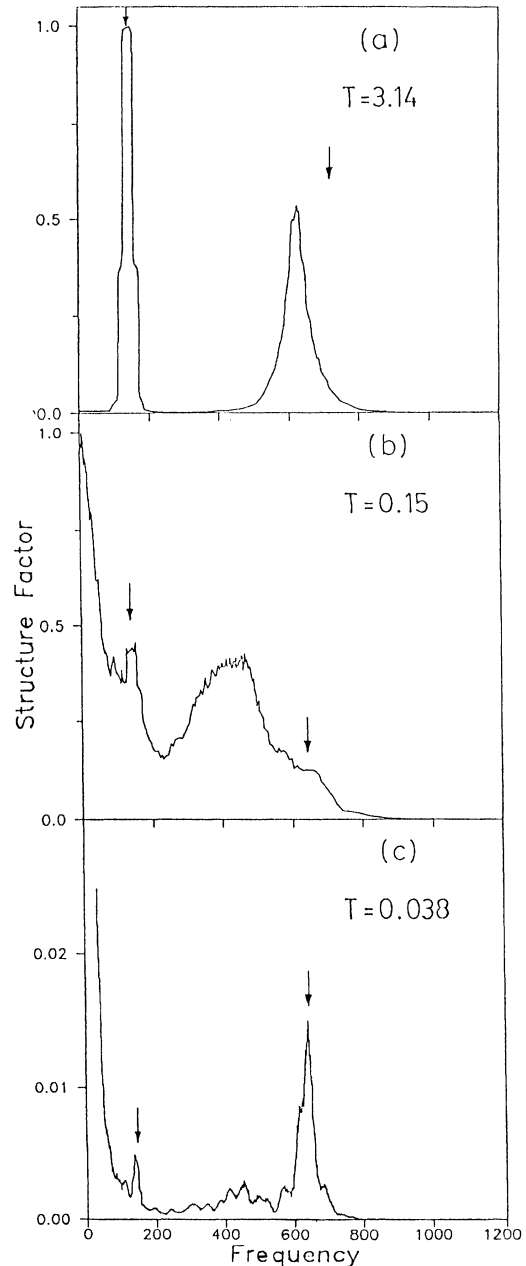


FIG. 2. The same as Fig. 1 but for  $q = \pi/a$ .

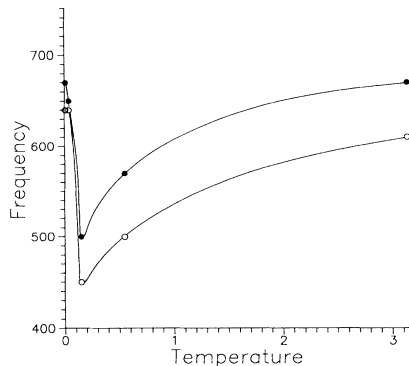


FIG. 3. Temperature dependence of the optical phonon peak as obtained from a molecular-dynamics simulation. Open circles correspond to  $q = \frac{3}{4}(\pi/a)$  and solid circles to  $q = \pi/a$ .

stant. In fact we have shown in the previous section some of the possible periodic minimal configurations and there may be even incommensurate solutions which would lead to a continuous structure in the quasistatic response. Such incommensurate configurations have been found in a similar nonlinear shell-model chain.<sup>10</sup> Features like the one we obtain in the quasistatic response have been found for the static structure factor from the static solutions for a chain with competitive nonlinear interactions.<sup>8</sup> Such interactions are not explicit in our model, but they are originated when the adiabatic condition is resolved in order to obtain an effective potential for the cores.

Now we will discuss the broad structure associated with the optic phonon at intermediate and low temperatures. The low-temperature spectrum of Fig. 2(c) shows a fairly well-defined structure below the optic peak, and the same feature, although less defined, is seen in Fig. 1(c). Also, a broad structure centered at about 400 and 500 frequency units in Figs. 2(b) and 1(b), respectively, seems to be differentiated from another broad structure at high frequencies, centered at the self-consistent phonon frequency. This may be a precursor effect of the low-

temperature behavior. This apparent additional structure could not be resolved more clearly, but a definite additional peak of the dynamical structure factor appears below the acoustic peak for a model parameter regime where the breathing mode corresponds to the acoustic branch.<sup>5</sup> Thus, the nonlinear breathing dynamic is capable of producing additional structures in the dynamic response to external fields. This allows one to explain the additional nonphononic peak observed in the neutron inelastic-scattering response of  $\text{La}_2\text{CuO}_4$ .<sup>5</sup> Also, the valence fluctuating system  $\text{Sm}_{0.75}\text{Y}_{0.25}\text{S}$  shows an additional branch<sup>2</sup> which cannot be ascribed to localized vibrations of the Y ion.<sup>6</sup> It has been explained in terms of a nonadiabatic breathing shell model with a damping term for the Sm breathing shell.<sup>11,12</sup> Our results suggest that the damping might be simulating the effect of the nonlinear core-shell coupling in our model, and the additional excitation may stem from the nonlinear dynamics.

In summary, we simulated the dynamics of a system with local charge fluctuations by means of a one-dimensional nonlinear breathing shell model. The response function obtained through a molecular-dynamics calculation differs significantly from the one corresponding to a linearized approximation. Upon decreasing temperature, the breathing phonon softens up to a finite frequency at a certain temperature where it becomes very broad, and then hardens and sharpens again. More striking is the appearance at low temperatures of a quasielastic peak from finite wavelengths up to the Brillouin-zone boundary. This behavior is originated by quasistatic structures with different periods than the reference lattice. Finally, at low temperatures, an additional structure due to nonlinear excitations appears at finite frequencies for a regime of parameters where the double-well potential barrier is higher than the intersite coupling.

#### ACKNOWLEDGMENTS

We thank S. Koval for useful discussions. A. D. and A. G. acknowledge support from CIUNR. R. M. and M. S. acknowledge support from CONICET.

<sup>1</sup>H. A. Mook and R. M. Nicklow, Phys. Rev. B **20**, 1656 (1979).  
<sup>2</sup>H. A. Mook, R. M. Nicklow, T. Penney, F. Holtzberg, and M. W. Shafer, Phys. Rev. B **18**, 2925 (1979).  
<sup>3</sup>N. Stüser, G. Güntherodt, A. Jayaraman, K. Fischer, and F. Holtzberg, in *Valence Instabilities*, edited by P. Wachter and H. Boppert (North-Holland, Amsterdam, 1982), p. 69.  
<sup>4</sup>L. Pintschovius, N. Pyka, W. Reichardt, A. Yu. Rumiantsev, A. Ivanov, and N. Mitrofanov, in *Progress in High Temperature Superconductivity*, edited by N. Bogoliubov, V. Aksenov, and N. Plakida (World Scientific, Singapore, 1990), Vol. 21, p. 36.  
<sup>5</sup>A. Dobry, A. Greco, R. Migoni, and M. Stachiotti, Solid State

Commun. **82**, 963 (1992).  
<sup>6</sup>H. Bilz, G. Güntherodt, W. Kleppmann, and W. Kress, Phys. Rev. Lett. **43**, 1998 (1979).  
<sup>7</sup>M. Miura and H. Bilz, Solid State Commun. **59**, 143 (1986).  
<sup>8</sup>T. Janssen and J. A. Tjon, Phys. Rev. B **25**, 3767 (1982).  
<sup>9</sup>T. Schneider and E. Stoll, Phys. Rev. B **23**, 4631 (1981).  
<sup>10</sup>H. Büttner and H. Bilz, J. Phys. (Paris) Colloq. **12**, C6-111 (1981).  
<sup>11</sup>G. Pastor, A. Caro, and B. Alascio, Solid State Commun. **56**, 497 (1985).  
<sup>12</sup>G. Pastor, A. Caro, and B. Alascio, Phys. Rev. B **36**, 1673 (1987).